Stability and collapse of fermions in a binary dipolar boson-fermion ^{164}Dy-^{161}Dy mixture

S. K. Adhikari*

Instituto de Física Teórica, UNESP-Universidade Estadual Paulista, 01.140-070 São Paulo, São Paulo, Brazil

(Received 6 May 2013; revised manuscript received 12 August 2013; published 3 October 2013)

We suggest a time-dependent mean-field hydrodynamic model for a binary dipolar boson-fermion mixture to study the stability and collapse of fermions in the ^{164}Dy-^{161}Dy mixture. The condition of stability of the dipolar mixture is illustrated in terms of phase diagrams. A collapse is induced in a disk-shaped stable binary mixture by jumping the interspecies contact interaction from repulsive to attractive by the Feshbach resonance technique. The subsequent dynamics is studied by solving the time-dependent mean-field model including three-body loss due to molecule formation in boson-fermion and boson-boson channels. Collapse and fragmentation in the fermions after subsequent explosions are illustrated. The anisotropic dipolar interaction leads to anisotropic fermionic density distribution during collapse. This study is carried out in three-dimensional space using realistic values of dipolar and contact interactions.

DOI: 10.1103/PhysRevA.88.043603 PACS number(s): 03.75.Hh, 03.75.Ss, 03.75.Kk, 05.30.Fk

I. INTRODUCTION

The alkali-metal atoms used in most Bose-Einstein condensation (BEC) experiments have negligible dipole moment. However, BECs of magnetically polarized atoms, for instance, ^{52}Cr [1], ^{168}Er [2], and ^{164}Dy [3] atoms, with reasonably large magnetic moments have been realized. Polar molecules with much larger electric dipole moments are also being considered for BEC experiments [4]. Thus, one can study the interplay between the long-range anisotropic dipolar interaction and a variable short-range interaction [1] using a Feshbach resonance [5] in a dipolar BEC. The stability of a dipolar BEC depends not only on the atomic interaction, but also strongly on trap geometry [1,6]. In a disk configuration, the dipolar interaction is repulsive and a dipolar BEC is more stable, while in a cigar configuration the dipolar interaction is attractive and a dipolar BEC is less stable due to collapse instability. A remarkable feature of the stability of a dipolar BEC is that, irrespective of the underlying trap symmetry, a dipolar BEC always becomes unstable to collapse with the increase of dipolar interaction or of the number of atoms [7–9]. This means that, in the disk shape with predominantly repulsive dipolar interaction, a dipolar BEC is unstable beyond a critical number of atoms even for repulsive short-range atomic interaction. This leads to peculiar stability phase diagrams for single-component [7,9] and binary dipolar [10] BECs. The controllable short-range interaction together with the long-range dipolar interaction make the dipolar BEC an attractive system for experimental study and a challenging system for theoretical investigation. Because of the peculiar features, there has been enhanced interest in the study of dynamic as well as static properties of dipolar BECs. Among the novel features of a dipolar BEC, one can mention the peculiar stability phase diagrams [6], red-blood-cell-like biconcave density distribution due to radial and angular rotonlike excitations [11], anisotropic D-wave collapse [12], formation of anisotropic soliton, vortex soliton [13] and vortex lattice [14], anisotropic shock and sound waves [15], entanglement [16], localization in disordered potential [17], and anisotropic Landau critical velocity [18] among others. Stable checkerboard, star, and stripe configurations in dipolar BECs have been identified in a two-dimensional (2D) optical lattice as stable Mott insulator [19] as well as superfluid soliton [20] states. A new possibility of studying universal properties of dipolar BECs at unitarity has been suggested [21].

After the pioneering experiments on BEC of alkali-metal atoms, degenerate spin-polarized gases of fermionic ^{6}Li [22], ^{40}K [23], and ^{87}Sr [24] atoms were observed. Later, superfluid states of paired ^{6}Li [25] and ^{40}K [26] atoms have also been studied. More recently, a degenerate dipolar gas of fermionic ^{161}Dy atoms with large magnetic moment has been created and studied [27]. Fermionic polar molecules, such as ^{40}K^{87}Rb, are also being considered for these studies [28]. With a dipole moment of 0.6 debye, the ^{40}K^{87}Rb molecule in the singlet rovibrational ground state has a dipolar interaction larger than in ^{161}Dy atoms by more than an order of magnitude [28,29]. A trapped degenerate spin-polarized nondipolar fermionic gas is absolutely stable for any number of atoms owing to strong Pauli repulsion among identical fermions. However, due to the peculiar nature of dipolar interaction, a trapped degenerate dipolar spin-polarized fermionic gas is unstable for the number of atoms above a critical value [9,30]. Although, the short-range S-wave contact interaction is absent in nondipolar fermionic gas, the dipolar interaction operative in the fermionic gas is responsible for the collapse instability.

Collapse dynamics in a nondipolar BEC of ^{85}Rb atoms, initiated by jumping the scattering length from positive (repulsive) to negative (attractive) near a Feshbach resonance [5], has revealed many fascinating novel features [31–33] such as jet formation and explosion after collapse. Although collapse is forbidden in a gas of degenerate trapped single-component nondipolar fermions in isolation due to Pauli repulsion among identical fermions, it is possible in a trapped degenerate boson-fermion mixture with attractive short-range boson-fermion interaction. There have been experimental [34] and theoretical [35] investigations of fermion collapse in a binary boson-fermion ^{87}Rb-^{40}K mixture. The presence of the bosons facilitates collapse via attractive interspecies interaction.

Recently, there has been interest in creating and studying a highly dipolar trapped boson-fermion mixture of dysprosium isotopes [3,27]. In the ^{164}Dy-^{161}Dy boson-fermion mixture, the

*adhikari@ift.unesp.br

presence of the bosonic ^{164}Dy atoms will favor the collapse in the fermionic ^{161}Dy atoms for attractive boson-fermion contact interaction. Hence, we study the statics and dynamics of collapse of fermionic ^{161}Dy atoms in the trapped binary ^{164}Dy-^{161}Dy mixture using a mean-field model. The stability of the mixture is illustrated by phase diagrams showing the critical number of ^{164}Dy atoms in the stable mixture for different values of intraspecies boson-boson and interspecies boson-fermion scattering lengths and for different trap aspect ratios. To study the dynamics of collapse, we include in our model two types of three-body loss by the formation of boson-boson and boson-fermion molecules. In the presence of these three-body losses we study the evolution of the number of ^{164}Dy and ^{161}Dy atoms during collapse. After the initial quick loss of a large number of atoms, quasistable bosonic and fermionic remnants are formed, which are found to last for a large interval of time. The three-dimensional (3D) isodensity contours of the remnants clearly exhibit the dynamics of fragmentation. The non-S-wave nature of the dipolar interaction is clearly seen in the 2D and 3D isodensity contours.

In Sec. II, we present the mean-field model for studying the statics and dynamics of the binary dipolar boson-fermion ^{164}Dy-^{161}Dy mixture. In this model, we incorporate all interspecies and intraspecies short-range S-wave and long-range dipolar interactions. Two possibilities of three-body loss by the formation of boson-boson ^{164}Dy^{164}Dy and boson-fermion ^{164}Dy^{161}Dy molecules are also included in the dynamics. In Sec. III, we report the results of numerical investigation. The stability of the system is demonstrated in terms of phase diagrams. We also present the results of dynamical evolution of the system during collapse and illustrate non-S-wave density distribution during collapse due to dipolar interaction. Finally, in Sec. IV, we present a brief summary of this study and future perspectives.

II. MEAN-FIELD HYDRODYNAMIC MODEL

We study the degenerate mixture of N_b bosonic atoms of mass m_b and N_f spin-up fermionic atoms of mass m_f under the action of interspecies and intraspecies isotropic short-range and anisotropic dipolar interactions at zero temperature. The bosonic atoms form a BEC, and superfluid P-wave pairing in the fermionic system occurs for dipolar interactions beyond a critical strength for a definite trap aspect ratio [36]. In the presence of superfluid pairing, the bosonic and fermionic superfluids are described by the order parameters Φ_b and Φ_f, respectively. In this hydrodynamic description of fermionic superfluid we neglect the gap and take the density $n_f = |\Phi_f|^2$, although the gap can be accommodated in an improved hydrodynamic model [37]. Assuming that the superfluidity in fermions has been achieved, we present the following mean-field model for the binary superfluid. However, if the parameters of the model, e.g., number of atoms, dipolar strength, trap aspect ratio, etc., are below the critical limit for attaining pairing in fermions, the present model will still be valid where Φ_f will not be the fermionic order parameter but should be related to the density n_f via $n_f = |\Phi_f|^2$. The fermionic system will then be in a collisional hydrodynamic regime [38] where the hydrodynamic behavior appears due to collision among the dipolar fermions possible in the presence of P-wave interaction. Unless we study rotational properties, e.g., quantized vortex formation, collisional hydrodynamic and superfluid phases can not be distinguished easily and will be described by the same hydrodynamics equations. A complete analysis to determine the critical limit of attaining fermion pairing in the binary dipolar boson-fermion mixture is beyond the scope of this study and here we only relate the function Φ_f to density and not to any other superfluid property of fermions. A similar interpretation of the fermionic function Φ_f in the normal fermionic gas has led a satisfactory description of the nondipolar boson-fermion mixture [35,39]. The correction due to anti-symmetrization of identical fermions can be included following the formalism of Ref. [9]. The correction is found to be negligible at low-densities considered in this paper and is not considered here.

The fermionic atoms are treated by a hydrodynamical Lagrangian and the bosonic atoms by the mean-field Gross-Pitaevskii Lagrangian. After including the dipolar interaction terms following Refs. [10,40] in the standard Lagrangian density of the boson-fermion mixture [41,42], the Euler-Lagrange equations for the binary mixture can be written as

$$
\begin{aligned}
i\hbar\frac{\partial\Phi_b(\mathbf{r},t)}{\partial t} &= \left[-\frac{\hbar^2}{2m_b}\nabla^2+\frac{1}{2}m_b\omega_b^2\left(\frac{\rho^2}{\lambda_b^{2/3}}+z^2\lambda_b^{4/3}\right)\right.\\
&+\frac{4\hbar^2\pi a_b}{m_b}|\Phi_b|^2+\frac{2\pi\hbar^2}{m_R}a_{bf}|\Phi_f|^2\\
&+\frac{\mu_0\mu_b^2}{4\pi}\int V_{dd}(\mathbf{r}-\mathbf{r}')|\Phi_b(\mathbf{r}')|^2d\mathbf{r}'\\
&\left.+\frac{\mu_0\mu_b\mu_f}{4\pi}\int V_{dd}(\mathbf{r}-\mathbf{r}')|\Phi_f(\mathbf{r}')|^2d\mathbf{r}'\right]\Phi_b(\mathbf{r},t), \quad (1)
\end{aligned}
$$

$$
\begin{aligned}
i\hbar\frac{\partial\Phi_f(\mathbf{r},t)}{\partial t} &= \left[-\frac{\hbar^2}{8m_f}\nabla^2+\frac{1}{2}m_f\omega_f^2\left(\frac{\rho^2}{\lambda_f^{2/3}}+z^2\lambda_f^{4/3}\right)\right.\\
&+\frac{\mu_0\mu_b\mu_f}{4\pi}\int V_{dd}(\mathbf{r}-\mathbf{r}')|\Phi_b(\mathbf{r}')|^2d\mathbf{r}'+\frac{2\pi\hbar^2}{m_R}a_{bf}|\Phi_b|^2\\
&\left.+\frac{\mu_0\mu_f^2}{4\pi}\int V_{dd}(\mathbf{r}-\mathbf{r}')|\Phi_f(\mathbf{r}')|^2d\mathbf{r}'+\mu_F\right]\Phi_f(\mathbf{r},t), \quad (2)
\end{aligned}
$$

with normalization $\int|\Phi_i(\mathbf{r})|^2d\mathbf{r}=N_i, i=b,f$, where we have included the dipolar interaction terms following Ref. [10]. The prefactor $-\hbar^2/8m_f$ in the space derivative term of the fermionic equation (2) takes into account the possibility of pairing in dipolar fermions and leads to a Galilei-invariant dynamics [41]. The space derivative terms have a quantum origin and are called the quantum pressure terms. In the absence of these terms, Eqs. (1) and (2) reduce to the classical hydrodynamic equations, while the fermionic equation (2) becomes the well-known local density approximation. In the absence of pairing in the normal state, the prefactor $-\hbar^2/8m_f$ was suggested by von Weizsäcker for a proper description of density [43]. Here, μ_0 is the permeability of free space, μ_b and μ_f are magnetic moments of bosons and fermions,

respectively, $V_{dd}(\mathbf{R}) = (1-3\cos^2\theta)/R^3$, $\mathbf{R} = \mathbf{r}-\mathbf{r}'$, $m_R = m_b m_f/(m_b+m_f)$, and θ is the angle between the vector $\mathbf{R}$ and the polarization direction z. The traps are axially symmetric for bosons and fermions with average angular frequencies ω_i and aspect ratios $\lambda_i = \omega_{zi}/\omega_{\rho i}$ with z and ρ denoting axial (polarization) and transverse directions, respectively: $\omega_i = (\omega_{\rho i}^2\omega_{zi})^{1/3}$. In Eq. (2), μ_F is the bulk chemical potential of the free spin-polarized fermionic gas

$$\mu_F = \frac{\hbar^2(6\pi^2|\Phi_f|^2)^{2/3}}{2m_f}. \tag{3}$$

Equations (1) and (2) are essentially the same as similar equations for a binary bosonic dipolar mixture [10] with the intraspecies contact interaction in the second bosonic component replaced by the fermionic bulk chemical potential μ_F.

To study the collapse dynamics in the dipolar boson-fermion mixture, we have to add the mechanisms for atom loss in Eqs. (1) and (2). The net interspecies boson-fermion and boson-boson interactions lead to the following three-body recombination processes to form boson-fermion (BF) and boson-boson (BB) molecules responsible for the loss of atoms [34]:

$$\mathrm{B}+\mathrm{B}+\mathrm{F} \rightarrow (\mathrm{BF})+\mathrm{B}, \tag{4}$$

$$\mathrm{B}+\mathrm{B}+\mathrm{F} \rightarrow (\mathrm{BB})+\mathrm{F}. \tag{5}$$

In addition, there is also the possibility of the formation of a boson-boson molecule by the reaction

$$\mathrm{B}+\mathrm{B}+\mathrm{B} \rightarrow (\mathrm{BB})+\mathrm{B}. \tag{6}$$

Although not prohibitive in the presence of dipolar interaction, we neglect the formation of a two-fermion molecule due to strong Pauli repulsion among identical spin-polarized fermions. For the same reason we also neglect the three-body loss initiated by a boson and two fermions or by three fermions. Consequently, fermionic atoms could only be lost in the presence of bosons according to reaction (4) and the loss rate scales quadratically with bosonic density and is independent of fermion number N_f [34]. There is also loss of bosonic atoms due to reactions (4)–(6). These reactions will contribute to imaginary (dissipative) loss terms in Eqs. (1) and (2). Of these, reaction (6) contributes to the loss term $-i\hbar K_3^{(bb)}|\Phi_b|^4/2$ in Eq. (1), reaction (4) contributes to the loss term $-i\hbar K_3^{(bf)}|\Phi_b|^2|\Phi_f|^2/2$ in Eq. (1) and $-i\hbar K_3^{(bf)}|\Phi_b|^4/2$ in Eq. (2), and reaction (5) contributes to a loss term $-i\hbar K_3^{(bbf)}|\Phi_b|^2|\Phi_f|^2/2$ in Eq. (1), where $K_3^{(bf)}$, $K_3^{(bbf)}$, and $K_3^{(bb)}$ are the respective loss rates of the reactions (4), (5), and (6), respectively. As the main interest of this study is to investigate the fermionic collapse, and as the experimental loss rates are not yet known, we combine contributions of bosonic loss terms of reactions (4) and (5) into a single term in Eq. (1).

To compare the dipolar and contact interactions, the intraspecies and interspecies dipolar interactions will be expressed in terms the lengths $a_{dd}^{(i)}$ $(i=b,f)$ and $a_{dd}^{(bf)}$, respectively, defined by

$$\frac{\mu_0\mu_i^2}{4\pi} = \frac{3\hbar^2}{m_i}a_{dd}^{(i)}, \quad \frac{\mu_0\mu_b\mu_f}{4\pi} = \frac{3\hbar^2}{2m_R}a_{dd}^{(bf)}. \tag{7}$$

We express the strengths of the dipolar interactions in Eqs. (1) and (2) by these dipolar lengths and transform these equations into the following dimensionless form:

$$\begin{aligned} i\frac{\partial\phi_b(\mathbf{r},t)}{\partial t} &= \Bigg[-\frac{\nabla^2}{2}+\frac{1}{2}\left(\frac{\rho^2}{\lambda_b^{2/3}}+\lambda_b^{4/3}z^2\right)+g_{bf}|\phi_f|^2 \\ &\quad + g_{dd}^{(b)}\int V_{dd}(\mathbf{R})|\phi_b(\mathbf{r}',t)|^2d\mathbf{r}' + g_b|\phi_b|^2 \\ &\quad + g_{dd}^{(bf)}\int V_{dd}(\mathbf{R})|\phi_f(\mathbf{r}',t)|^2d\mathbf{r}' \\ &\quad - \frac{i}{2}k_3^{(bb)}N_b^2|\phi_b|^4 - \frac{i}{2}k_3^{(bf)}N_bN_f|\phi_b|^2|\phi_f|^2\Bigg]\phi_b(\mathbf{r},t), \end{aligned} \tag{8}$$

$$\begin{aligned} i\frac{\partial\phi_f(\mathbf{r},t)}{\partial t} &= \Bigg[-m_{bf}\frac{\nabla^2}{8}+\frac{m_w}{2}\left(\frac{\rho^2}{\lambda_f^{2/3}}+\lambda_f^{4/3}z^2\right) \\ &\quad + g_{dd}^{(f)}\int V_{dd}(\mathbf{R})|\phi_f(\mathbf{r}',t)|^2d\mathbf{r}' \\ &\quad + \frac{m_{bf}}{2}(6\pi^2N_f|\phi_f|^2)^{2/3} + g_{fb}|\phi_b|^2 \\ &\quad + g_{dd}^{(fb)}\int V_{dd}(\mathbf{R})|\phi_b(\mathbf{r}',t)|^2d\mathbf{r}' \\ &\quad - \frac{i}{2}k_3^{(bf)}N_b^2|\phi_b|^4\Bigg]\phi_f(\mathbf{r},t), \end{aligned} \tag{9}$$

with normalization $\int|\phi_i(\mathbf{r})|^2d\mathbf{r}=1$, where $m_{bf} = m_b/m_f$, $m_w = \omega_f^2/(m_{bf}\omega_b^2)$, $g_b = 4\pi a_b N_b$, $g_{dd}^{(b)} = 3N_b a_{dd}^{(b)}$, $g_{bf} = 2\pi m_b a_{bf} N_f/m_R$, $g_{fb} = 2\pi m_b a_{bf} N_b/m_R$, $g_{dd}^{(f)} = 3N_f a_{dd}^{(f)}$ $m_{bf}, g_{dd}^{(bf)} = 3N_f a_{dd}^{(bf)}(m_b/2m_R), g_{dd}^{(fb)} = 3N_b a_{dd}^{(bf)}(m_b/2m_R)$. In Eqs. (8) and (9), length is expressed in units of oscillator length for boson $l_0 = \sqrt{\hbar/m_b\omega}$, energy and chemical potential in units of oscillator energy $\hbar\omega$, density $|\phi_i|^2$ in units of l_0^{-3}, and time in units of $t_0 = \omega^{-1}$, with $\omega \equiv \omega_b$, $k_3^{(bf)} \equiv K_3^{(bf)}/(\omega_b l_0^6)$, and $k_3^{(bb)} \equiv K_3^{(bb)}/(\omega_b l_0^6)$ are the dimensionless three-body loss rates for the formation of (BF) and (BB) molecules.

III. NUMERICAL RESULTS

We perform numerical calculation for the stability and dynamics of the binary dipolar ^{164}Dy-^{161}Dy boson-fermion mixture using realistic values of the parameters. We solve the dynamical equations (8) and (9) by the split-step Crank-Nicolson method [44], in 3D Catesian coordinates independent of the trap symmetry using a space step of $0.1 \sim 0.2$ and time step of $0.001 \sim 0.003$. For the fermionic system of ^{161}Dy atoms, we take the trap frequencies $f_f = \{180,200,720\}$ Hz corresponding to the geometrical mean angular frequency of $\omega_f = 2\pi \times 296$ Hz and trap aspect ratio $\lambda_f = 3.8$ as used in the recent experiment [27]. For the BEC of ^{164}Dy atoms we take the trap frequencies $f_b = \{195,205,760\}$ Hz corresponding to the geometrical mean angular frequency of $\omega_b = 2\pi \times 312$ Hz and trap aspect ratio $\lambda_b = 3.8$ as in the experiment [3]. The bosonic oscillator length $l_0 = \sqrt{\hbar/m_b\omega_b} = 0.443$ μm and the fermionic oscillator length $\sqrt{\hbar/m_f\omega_f} = 0.459$ μm. The Dy atoms have a large magnetic dipole moment $\mu = 10\mu_B$

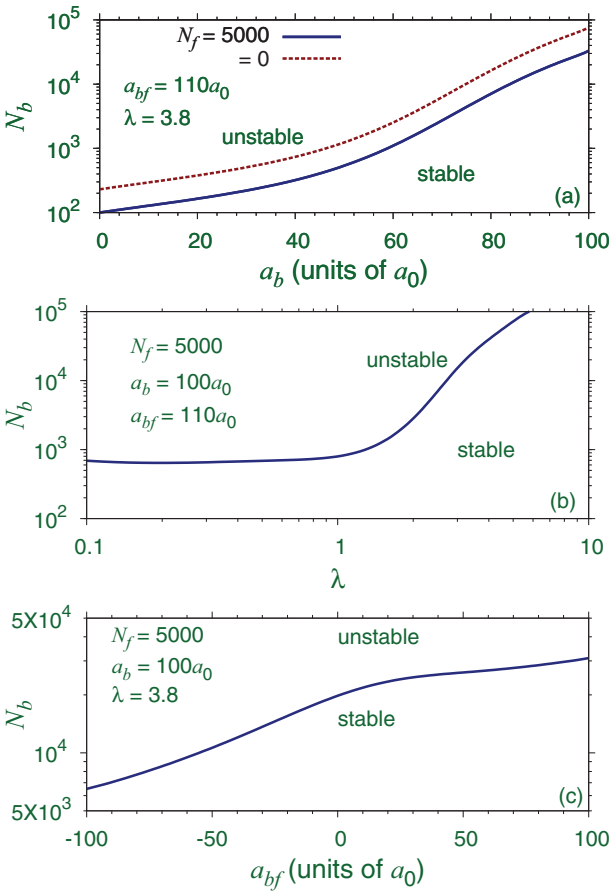

FIG. 1. (Color online) (a) Stability phase diagram of the number of bosonic ^{164}Dy atoms N_b versus bosonic scattering length a_b for the binary ^{164}Dy-^{161}Dy mixture for the number of fermionic ^{161}Dy atoms $N_f = 0$, 5000, and for the interspecies scattering length $a_{bf} = 110a_0$. (b) Stability phase diagram of N_b versus λ for $N_f = 5000$, $a_{bf} = 110a_0$, and $a_b = 100a_0$. (c) Stability phase diagram of N_b versus a_{bf} for $N_f = 5000$, $a_b = 100a_0$. Dipolar lengths a_{dd} are taken as $a_{dd}^{(b)} = 132.7a_0$, $a_{dd}^{(f)} = 130.3a_0$, and $a_{dd}^{(bf)} = 131.5a_0$ and oscillator length scale $l_0 = 0.443$ μm.

with μ_B ($= 9.27402 \times 10^{-24}$ m^2 A) the Bohr magneton corresponding to the dipolar lengths $a_{dd}^{(b)} \equiv \mu_0\mu^2 m_b/(12\pi\hbar^2) \approx 132.7a_0$ for ^{164}Dy, $a_{dd}^{(f)} \equiv \mu_0\mu^2 m_f/(12\pi\hbar^2) \approx 130.3a_0$ for ^{161}Dy, and $a_{dd}^{(bf)} \equiv \mu_0\mu^2 m_R/(6\pi\hbar^2) \approx 131.5a_0$, with a_0 ($= 5.29 \times 10^{-11}$ m) the Bohr radius, $\mu_0 = 4\pi \times 10^{-7}$ N/A^2, $\hbar = 1.05457 \times 10^{-34}$ m^2 kg s, 1 amu $= 1.66054 \times 10^{-27}$ kg. Thus, the dipolar interaction in Dy atoms is more than eight times larger than that in Cr atoms with a dipolar length $a_{dd} \approx 15a_0$ [1].

In this study on the dynamics of collapse the bosonic scattering length a_b is taken as $100a_0$. First, we study the stability of the binary dipolar boson-fermion mixture for a fixed total number of fermions $N_f = 5000$ and illustrate the results in Fig. 1 through phase diagrams showing the critical number of bosons N_b in a stable boson-fermion mixture versus (a) the bosonic scattering length a_b, (b) trap aspect ratio $\lambda = \lambda_b = \lambda_f$, and (c) the boson-fermion scattering length a_{bf} keeping other variables fixed at constant values, e.g., (a) $a_{bf} = 110a_0$, $\lambda = 3.8$, (b) $a_{bf} = 110a_0$, $a_b = 100a_0$, and (c) $a_b = 100a_0$, and $\lambda = 3.8$. Because of the strong interspecies and intraspecies dipolar interactions, the binary mixture becomes unstable beyond a total number of atoms, independent of the other parameters, as shown in Fig. 1. To identify the region of instability of the binary system, time evolution with dynamical equations (1) and (2) is carried to very large time (about 50 to 100 units of time). The system is considered stable if this procedure leads to finite converged densities. Similar instability for larger net dipolar interaction was noted in case of both single-component [1,7] and binary [10] dipolar BEC. The increased repulsion for larger intraspecies and interspecies contact interactions appearing for large values of a_b or a_{bf}, respectively, favors stability, and hence can accommodate a larger number of ^{164}Dy atoms as can be seen in Figs. 1(a) and 1(c). For fixed values of contact interactions, a disk shape favors stability as can be seen in Fig. 1(b). The phase diagram for $N_f = 0$ in Fig. 1(a) reveals that the extra dipolar interaction in the boson-fermion mixture makes the system more vulnerable to collapse for repulsive contact interactions, when compared with the pure bosonic system.

It is known that, unlike the nondipolar degenerate fermion gas, the polarized dipolar fermion gas collapses for increased dipolar interaction [30]. But, the tendency to collapse is much enhanced in the dipolar boson-fermion mixture in the presence of attractive interspecies interaction. Hence, to study the collapse dynamics in the boson-fermion mixture, we introduce instability by suddenly changing the interspecies contact interaction from repulsive to attractive which can be achieved by varying a background magnetic field near a Feshbach resonance [5]. A similar variation of the interspecies contact interaction from repulsive to attractive has been demonstrated to lead to a net attraction in an otherwise repulsive binary mixture resulting in soliton formation [45] and collapse [46]. During collapse we maintain all the dipolar interactions and the intraspecies bosonic interaction at the respective initial values. From Fig. 1(c) we find that a larger number of about 30 000 ^{164}Dy atoms can be accommodated for $a_{bf} = 100a_0$ than about 6000 ^{164}Dy atoms for $a_{bf} = -100a_0$. Hence, for the study of collapse dynamics we consider an initial mixture of 20 000 ^{164}Dy atoms and 5000 ^{161}Dy atoms and initiate collapse by suddenly jumping the interspecies scattering length a_{bf} from $100a_0$ to $-100a_0$. From Fig. 1(c) we find that at $a_{bf} = -100a_0$ the binary dipolar mixture of 20 000 ^{164}Dy atoms and 5000 ^{161}Dy atoms becomes unstable to collapse. It is pertinent to mention that the same binary boson-fermion system with all dipolar interactions set to zero is absolutely stable and does not collapse even for the attractive interspecies scattering length $a_{bf} = -100a_0$. Hence, the collapse studied here is caused solely by the dipolar interaction. This is further substantiated by the higher-partial-wave shape in density distribution in Fig. 5. The numerical simulation was carried out in a sufficiently large 3D box of size $38 \times 38 \times 25$ and there was no reflection of matter wave from the boundary.

For the study of the collapse dynamics we have to fix the values of three-body loss rates $k_3^{(bb)}$ and $k_3^{(bf)}$ in Eqs. (8) and (9). We did the calculation for three sets of dimensionless loss rates: (i) $k_3^{(bb)} = 0.00005$ and $k_3^{(bf)} = 0.0001$, (ii) $k_3^{(bb)} = 0.0005$ and $k_3^{(bf)} = 0.001$, and (iii) $k_3^{(bb)} = 0.00001$ and $k_3^{(bf)} = 0.00004$.

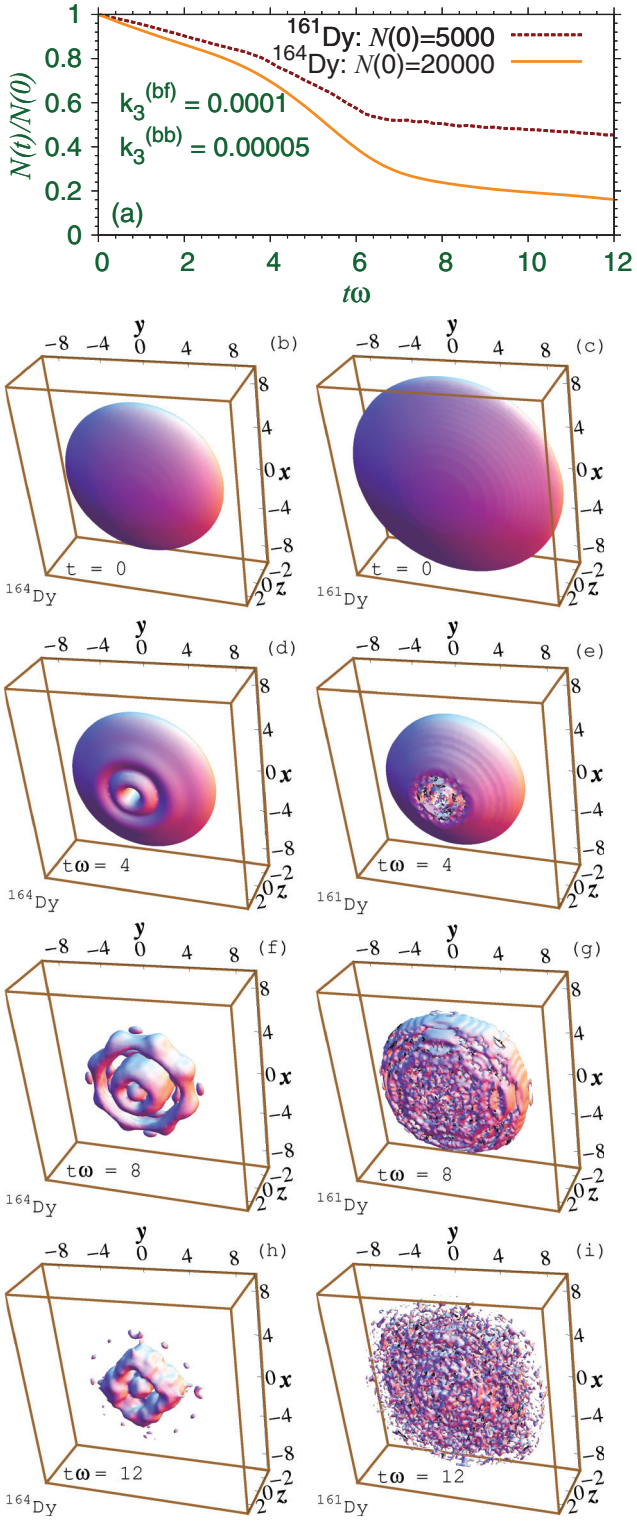

FIG. 2. (Color online) (a) Relative number of atoms $N(t)/N(0)$ versus time during collapse of a binary mixture of 20 000 ^{164}Dy and 5000 ^{161}Dy atoms initiated by jumping a_{bf} from $100a_0$ to $-100a_0$. Isodensity profile of ^{164}Dy and ^{161}Dy atoms at (dimensionless) times $t\omega = 0$, 4, 8, 12 are shown in (b)–(h). Parameters used $a_{dd}^{(b)} = 132.7a_0$, $a_{dd}^{(f)} = 130.3a_0$, $a_{dd}^{(bf)} = 131.5a_0$, $a_b = 100a_0$, $\lambda = 3.8$, $K_3^{(bb)} = 7.5 \times 10^{-28}$ cm^6 s, $K_3^{(bf)} = 1.5 \times 10^{-27}$ cm^6 s, density on contour 0.0005, and $\omega \equiv \omega_b$. Lengths and densities are in units of oscillator length l_0 and l_0^{-3}.

These correspond to the following physical loss rates: (i) $K_3^{(bb)} \equiv k_3^{(bb)}\omega_b l_0^6 = 7.5 \times 10^{-28}$ cm^6 s and $K_3^{(bf)} \equiv k_3^{(bf)}\omega_b l_0^6 = 1.5 \times 10^{-27}$ cm^6 s; (ii) $K_3^{(bb)} = 7.5 \times 10^{-27}$ cm^6 s and $K_3^{(bf)} = 1.5 \times 10^{-26}$ cm^6 s; and (iii) $K_3^{(bb)} = 1.5 \times 10^{-28}$ cm^6 s and $K_3^{(bf)} = 6 \times 10^{-28}$ cm^6 s; where we used $\omega_b = \omega = 2\pi \times 312$ Hz and $l_0 = 0.443$ μm. In the absence of accurate experimental numbers for these loss rates, we use these sets of values which seem to be quite realistic and comparable to the known experimental rates for other atoms. For example, for dipolar ^{52}Cr atoms the loss rate $K_3 = 2 \times 10^{-28}$ cm^6 s was used [12], in a ^{87}Rb-^{40}K boson-fermion mixture a loss rate of $K_3 = 2 \times 10^{-27}$ cm^6 s was measured [34], and for ^{85}Rb atoms the experimental loss rate was $K_3 \approx 5 \times 10^{-25}$ cm^6 s [47]. As the collapse dynamics of the binary mixture could be sensitive to loss rate, the three rates (i), (ii), and (iii) chosen here correspond to medium, strong, and mild loss rates, respectively. The collapse dynamics is expected to be distinct as the loss rates are changed from mild to strong and this fact motivates the study with the three rates above. The third set (iii) with the smallest loss rates produces a slower atom loss in the beginning and larger final residual remnant states after the collapse. The second set (ii) with the largest loss rates leads to a faster atom loss in the beginning and smaller final residual remnant states. The above sets of loss rates lead to a sizable amount of atom loss in less than 10 units of time as in the collapse of a nondipolar BEC of ^{85}Rb atoms [31].

In Fig. 2, we present the results of collapse dynamics with the first set of the rate parameters, e.g., $K_3^{(bb)} = 7.5 \times 10^{-28}$ cm^6 s, $K_3^{(bf)} = 1.5 \times 10^{-27}$ cm^6 s, for the binary mixture of 20 000 ^{164}Dy atoms and 5000 ^{161}Dy atoms. The collapse is initiated by jumping the interspecies scattering length a_{bf} from $100a_0$ to $-100a_0$. In Fig. 2(a), we show the time evolution of the number of bosonic and fermionic atoms $N(t)/N(0)$ during collapse. Due to a rapid initial three-body loss during collapse, the number of both bosonic and fermionic atoms reduces with time and after the initial loss of a significant fraction of atoms the rate of loss of atoms is much reduced and a remnant condensate is formed which survives for a long period of time as in the collapse of a single-component nondipolar BEC [31]. To visualize the collapse dynamics closely, we study the 3D isodensity contours of the condensates. In Figs. 2(b) and 2(c), we show the initial disk-shaped profiles of the bosonic and fermionic condensates. In Figs. 2(d)–2(i), we illustrate the profiles of the bosonic and fermionic condensates at times $t\omega = 4$, 8, and 12. The evolutions of bosonic and fermionic profiles are distinct. In the radial plane, the dipolar BEC develops maxima and minima due to dominant dipolar interaction. Similar maxima and minima were found to appear in binary dipolar BEC near the onset of instability due to increased dipolar interaction [10]. In Fig. 2, we find that the bosons maintain smooth profiles during collapse and atom loss, whereas the fermions experience violent dynamics and pass through unsmooth profiles. In this case, a sequence of collapse (with an increase in central density) and explosion (with a decrease in central density) starts at about $t\omega = 4$. Subsequently, after the repeated explosions, small fermionic fragments scatter all around and the fermions occupy a larger region in space as can be seen in Fig. 2(i) at $t\omega = 12$.

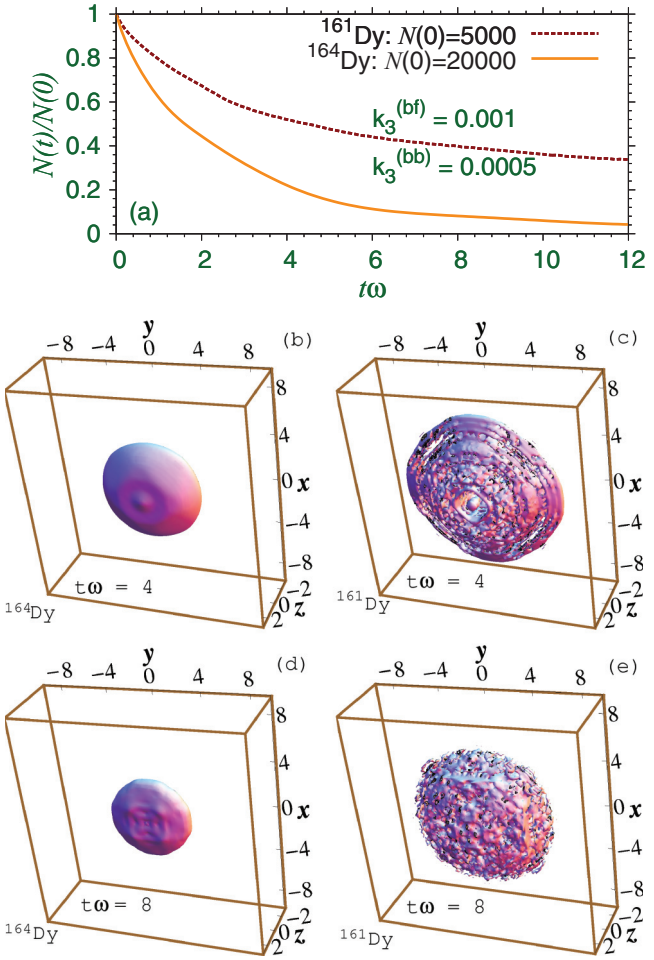

FIG. 3. (Color online) (a) Same as in Fig. 2(a) for loss rates $K_3^{(bb)} = 7.5 \times 10^{-27}$ cm^6 s, $K_3^{(bf)} = 1.5 \times 10^{-26}$ cm^6 s. Isodensity profile of ^{164}Dy and ^{161}Dy atoms at times $t\omega = 4,8$ are shown in (b)–(e) for these loss rates. Other parameters are the same as in Fig. 2.

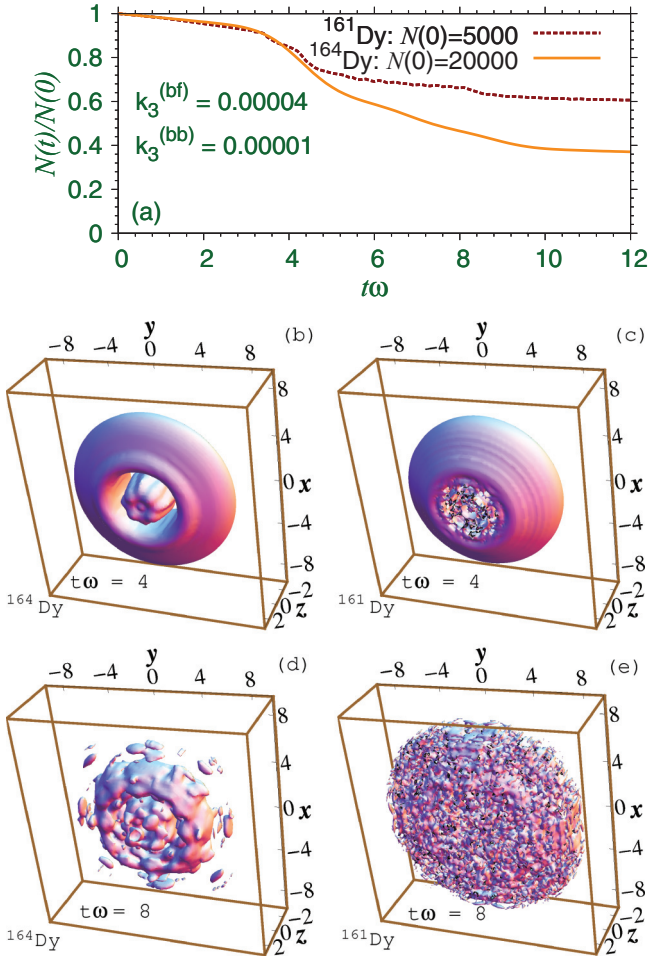

FIG. 4. (Color online) (a) Same as in Fig. 2(a) for loss rates $K_3^{(bb)} = 1.5 \times 10^{-28}$ cm^6 s, $K_3^{(bf)} = 6 \times 10^{-28}$ cm^6 s. Isodensity profile of ^{164}Dy and ^{161}Dy atoms at times $t\omega = 4,8$ are shown in (b)–(e) for these loss rates. Other parameters are the same as in Fig. 2.

In Fig. 3, we present the results of fermionic collapse in the binary mixture for the second set of rate parameters, e.g., $K_3^{(bb)} = 7.5 \times 10^{-27}$ cm^6 s, $K_3^{(bf)} = 1.5 \times 10^{-26}$ cm^6 s. The collapse is again initiated by jumping the interspecies scattering length a_{bf} from $100a_0$ to $-100a_0$. In Fig. 3(a), we show the time evolution of the number of atoms during collapse. The larger loss rates in this case compared to those used in Fig. 2 result in a more rapid loss of atoms in the beginning and smaller remnant condensates in the end. In case of the collapse of a single-component nondipolar BEC, it was also noted that a rapid initial loss of atoms leads to a smaller remnant BEC [31,32]. The initial profiles of the condensates in this case are the same as in Figs. 2(b) and 2(c) for bosons and fermions, respectively. The time evolution of the isodensity contours are shown in Figs. 3(b)–3(e) at times $t\omega = 4$ and 8. In this case, the dipolar BEC collapses towards the center and occupies a smaller central region after the onset of collapse. After atom loss, the bosonic profile continues smooth. However, the mark of collapse and explosion is more prominent in the case of fermions. The fermionic profile becomes unsmooth and small granules of matter are visible in this case.

In Fig. 4, we present the results of fermionic collapse in the binary mixture for the third set of loss rates, e.g., $K_3^{(bb)} = 1.5 \times 10^{-28}$ cm^6 s, $K_3^{(bf)} = 6 \times 10^{-28}$ cm^6 s, for collapse initiated by jumping the interspecies scattering length a_{bf} from $100a_0$ to $-100a_0$. This case corresponds to the smallest loss rates. Consequently, in this case the remnant states after long time are the largest in size as can be seen in Fig. 4(a). The time evolution of the profiles are shown in Figs. 4(b)–4(e) at times $t\omega = 4$ and 8. The profiles at $t\omega = 4$ are particularly interesting: the BEC ^{164}Dy has a Saturn-ring-type profile while the Fermi ^{161}Dy has a biconcave red-blood-cell-type profile. Similar structures were observed in a disk-shaped binary dipolar BEC on the verge of collapse and are a clear manifestation of dipolar interactions [10]. The sign of collapse and explosion is visible in the Fermi profile at $t\omega = 4$. At $t\omega = 8$, the explosion and fragmentation are more clearly seen in both profiles.

During collapse of the fermions, the non-S-wave shape due to dipolar interaction appears in the fermionic profiles. To illustrate, we show in Figs. 5(a) and 5(b) the contour plot of the effective 2D density $|\phi(x,z,t)|^2 \equiv \int dy |\phi(\mathbf{r},t)|^2$ in the x-z plane for the bosonic ^{164}Dy and fermionic ^{161}Dy

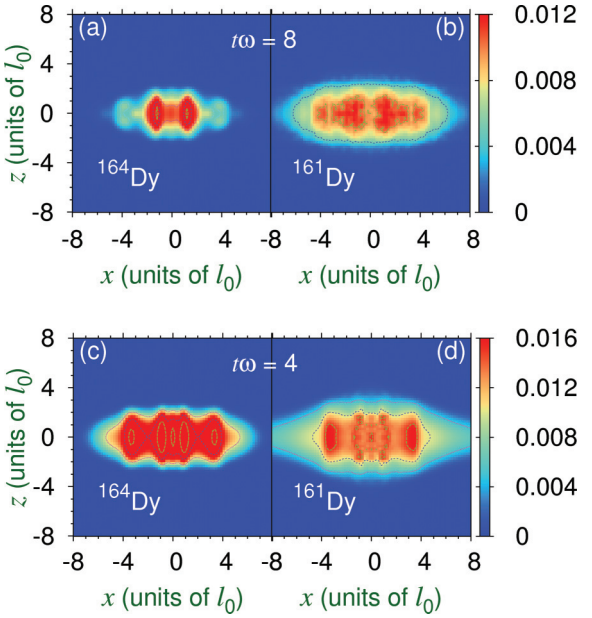

FIG. 5. (Color online) Effective 2D density of (a) ^{164}Dy and (b) ^{161}Dy atoms in the x-z plane $|\phi(x,z,t)|^2 \equiv \int dy|\phi(\mathbf{r},t)|^2$ in units of l_0^{-2} at (dimensionless) time $t\omega = 8$ for the dynamics shown in Figs. 2(f) and 2(g), respectively. The same of (c) ^{164}Dy and (d) ^{161}Dy atoms at time $t\omega = 4$ for the dynamics shown in Figs. 4(b) and 4(c), respectively.

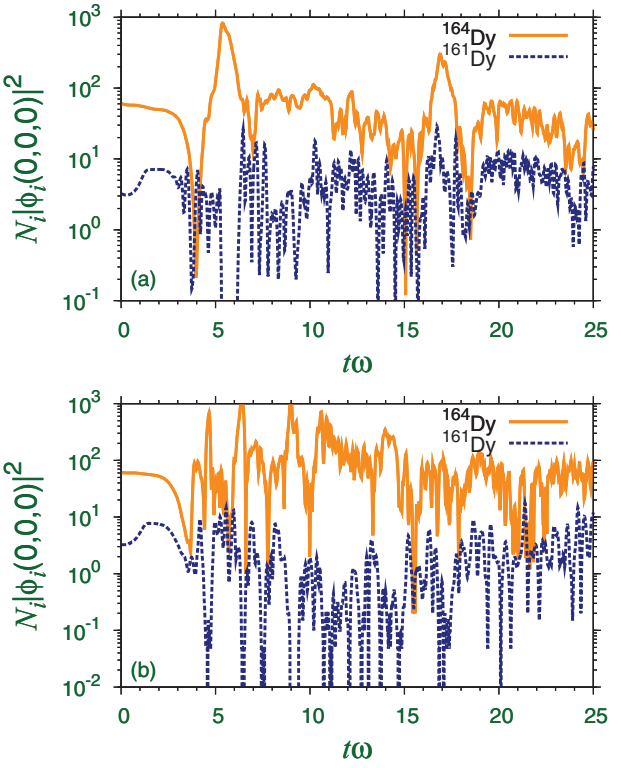

FIG. 6. (Color online) Time evolution of the central density $N_i|\phi_i(0,0,0)|^2$ in units of l_0^{-3} of the bosonic ^{164}Dy and fermionic ^{161}Dy atoms during collapse and explosion illustrated in (a) Fig. 2 and (b) Fig. 4.

atoms, respectively, during the dynamics shown in Figs. 2(f) and 2(g) at time $t\omega = 8$. Both profiles for density are found to exhibit higher partial-wave shape due to dipolar interaction. In Figs. 5(c) and 5(d), we show the contour plot of the effective 2D density $|\phi(x,z,t)|^2$ for the bosonic ^{164}Dy and fermionic ^{161}Dy atoms, respectively, during the dynamics shown in Figs. 4(b) and 4(c) at time $t\omega = 4$. The profile of the fermionic ^{161}Dy atoms in Figs. 5(b) and 5(d) is found to exhibit higher partial-wave shape due to dipolar interaction. The higher partial-wave shape in bosonic ^{164}Dy atoms also appears in Figs. 5(a) and 5(c). The saddle-point [48] structures in density in the x-z plane in Fig. 5 are manifestations of the dipolar interaction. In these plots, a minimum in density along the orthogonal x direction coincides with a maximum in density in the polarization z direction thus creating a saddle point, which appears as a clear manifestation of the saddle-shaped dipolar interaction [48]. The dipolar interaction leads to an effective trap with similar saddle shape [48]. Such a density distribution is not possible in the absence of dipolar interaction and also appears in a binary dipolar BEC [10]. Similar non-S-wave density distribution was also noted in the study of collapse of a dipolar BEC of ^{52}Cr atoms [12] due to a direct manifestation of dipolar interaction.

In Figs. 6(a) and 6(b) we show the evolution of central density $N_i|\phi_i(0,0,0)|^2$ of the bosonic ^{164}Dy and fermionic ^{161}Dy atoms during collapse and explosion illustrated in Figs. 2 and 4. The repeated collapse to center and subsequent explosion appear as the rapid increase and decrease in the central density, respectively. The collapse and explosion in the fermions is found to be more vigorous with rapid fluctuation in central density in the fermions than in the bosons in both cases. The reason is that the interspecies attractive contact interaction responsible for collapse acting on 5000 fermions due to 20 000 bosons is much stronger than the same acting on 20 000 bosons due to 5000 fermions. Consequently, fluctuation in the central density in the dipolar BEC of ^{164}Dy atoms is smoother than that in the fermionic ^{161}Dy atoms. In the dynamics presented in Fig. 6, after a smooth evolution of the binary system until $t\omega \approx 3$, the cycle of collapse and explosion starts with a rapid fluctuation of the central densities. Similar fluctuation of central densities was noted in the study of collapse of a nondipolar boson-fermion ^{87}Rb-^{40}K mixture [35].

IV. SUMMARY AND DISCUSSION

Matter built of identical fermions is stable against collapse in the presence of isotropic short-range interaction due to a strong Pauli repulsion. On the other hand, bosons can exhibit collapse instability for attractive interactions [31]. The phenomenon of collapse and explosion in bosonic atoms has been observed [31] and studied [32,33] in bosonic superfluids. However, it has been possible to observe collapse in fermions in the presence of bosons via an attractive interspecies isotropic short-range interaction [34]. It is also possible to have collapse instability in fermions in the presence of an anisotropic long-range dipolar interaction [9] operative in identical polarized fermions: the isotropic short-range interaction is forbidden in this case due to Pauli principle. Here, we considered a more favorable situation of the collapse of fermions in a binary boson-fermion mixture including dipolar

interaction as well as an attractive short-range boson-fermion interaction.

Because of recent experimental activities in a highly dipolar binary mixture of Dy isotopes [3,27], we studied fermionic collapse in the disk-shaped boson-fermion ^{164}Dy-^{161}Dy mixture. The stability of the mixture was illustrated using phase diagrams of an allowed critical number of bosonic ^{164}Dy atoms in the binary mixture for different short-range interspecies and intraspecies interactions as well as for different trap aspect ratios. The collapse was started in a stable mixture by jumping the interspecies scattering length from a positive (repulsive) to negative (attractive) value using a Feshbach resonance [5]. During collapse we include appropriate three-body loss rates via the formation of boson-boson and boson-fermion molecules. The evolution of the condensates during collapse was quantified by the evolution of respective atom numbers. The condensates first reduce in size rapidly by losing atoms via three-body loss and eventually become smaller remnant condensates which survive for a longer period of time. Such remnant condensates were observed in the collapse of nondipolar ^{85}Rb BEC [31]. We also identify anisotropic shapes of the condensates during collapse, which is a clear manifestation of dipolar interaction. The repeated collapse and explosion of the binary system were identified by rapidly oscillating central densities of the bosonic and fermionic atoms. After repeated collapse and explosion, small fermionic fragments appear covering the whole region. All calculations in this paper are performed with realistic values of the parameters and could be verified in future experiments.

ACKNOWLEDGMENT

We thank FAPESP and CNPq (Brazil) for partial support.

[1] T. Koch *et al*., Nat. Phys. **4**, 218 (2008); T. Lahaye *et al*., Nature (London) **448**, 672 (2007); A. Griesmaier, J. Stuhler, T. Koch, M. Fattori, T. Pfau, and S. Giovanazzi, Phys. Rev. Lett. **97**, 250402 (2006).

[2] K. Aikawa, A. Frisch, M. Mark, S. Baier, A. Rietzler, R. Grimm, and F. Ferlaino, Phys. Rev. Lett. **108**, 210401 (2012).

[3] M. Lu, N. Q. Burdick, S. H. Youn, and B. L. Lev, Phys. Rev. Lett. **107**, 190401 (2011).

[4] J. Deiglmayr, A. Grochola, M. Repp, K. Mörtlbauer, C. Glück, J. Lange, O. Dulieu, R. Wester, and M. Weidemüller, Phys. Rev. Lett. **101**, 133004 (2008); M. H. G. de Miranda *et al*., Nat. Phys. **7**, 502 (2011).

[5] S. Inouye *et al*., Nature (London) **392**, 151 (1998).

[6] N. G. Parker, C. Ticknor, A. M. Martin, and D. H. J. O'Dell, Phys. Rev. A **79**, 013617 (2009); R. M. Wilson, S. Ronen, and J. L. Bohn, *ibid*. **80**, 023614 (2009); N. G. Parker and D. H. J. O'Dell, *ibid*. **78**, 041601 (2008); S. Yi and L. You, *ibid*. **61**, 041604 (2000); C. Ticknor, N. G. Parker, A. Melatos, S. L. Cornish, D. H. J. O'Dell, and A. M. Martin, *ibid*. **78**, 061607 (2008); R. M. W. van Bijnen, A. J. Dow, D. H. J. O'Dell, N. G. Parker, and A. M. Martin, *ibid*. **80**, 033617 (2009); A. Junginger, J. Main, G. Wunner, and T. Bartsch, *ibid*. **86**, 023632 (2012).

[7] S. Ronen, D. C. E. Bortolotti, and J. L. Bohn, Phys. Rev. Lett. **98**, 030406 (2007).

[8] S. Yi and L. You, Phys. Rev. A **63**, 053607 (2001).

[9] S. K. Adhikari, J. Phys. B: At., Mol. Opt. Phys. **46**, 235303 (2013).

[10] Luis E. Young-S. and S. K. Adhikari, Phys. Rev. A **86**, 063611 (2012).

[11] R. M. Wilson, S. Ronen, J. L. Bohn, and H. Pu, Phys. Rev. Lett. **100**, 245302 (2008); M. Asad-uz-Zaman and D. Blume, Phys. Rev. A **83**, 033616 (2011).

[12] T. Lahaye, J. Metz, B. Frohlich, T. Koch, M. Meister, A. Griesmaier, T. Pfau, H. Saito, Y. Kawaguchi, and M. Ueda, Phys. Rev. Lett. **101**, 080401 (2008).

[13] I. Tikhonenkov, B. A. Malomed, and A. Vardi, Phys. Rev. Lett. **100**, 090406 (2008); S. K. Adhikari and P. Muruganandam, J Phys. B: At., Mol. Opt. Phys. **45**, 045301 (2012); L. E. Young-S., P. Muruganandam, and S. K. Adhikari, *ibid*. **44**, 101001 (2011); P. Muruganandam and S. K. Adhikari, *ibid*. **44**, 121001 (2011); P. Köberle, D. Zajec, G. Wunner, and B. A. Malomed, Phys. Rev. A **85**, 023630 (2012).

[14] R. M. W. van Bijnen, D. H. J. O'Dell, N. G. Parker, and A. M. Martin, Phys. Rev. Lett. **98**, 150401 (2007); R. Kishor Kumar and P. Muruganandam, J. Phys. B: At., Mol. Opt. Phys. **45**, 215301 (2012); R. Kishor Kumar, P. Muruganandam, and B. A. Malomed, *ibid*. **46**, 175302 (2013).

[15] P. Muruganandam and S. K. Adhikari, Phys. Lett. A **376**, 480 (2012); C. Krumnow and A. Pelster, Phys. Rev. A **84**, 021608 (2011).

[16] L. Dell'Anna, G. Mazzarella, V. Penna, and L. Salasnich, Phys. Rev. A **87**, 053620 (2013).

[17] B. Nikolić, Antun Balaž, and A. Pelster, Phys. Rev. A **88**, 013624 (2013); P. Muruganandam, R. K. Kumar, and S. K. Adhikari, J. Phys. B: At., Mol. Opt. Phys. **43**, 205305 (2010); C. Krumnow and A. Pelster, Phys. Rev. A **84**, 021608(R) (2011).

[18] R. M. Wilson, S. Ronen, and J. L. Bohn, Phys. Rev. Lett. **104**, 094501 (2010).

[19] B. Capogrosso-Sansone, C. Trefzger, M. Lewenstein, P. Zoller, and G. Pupillo, Phys. Rev. Lett. **104**, 125301 (2010).

[20] S. K. Adhikari and P. Muruganandam, Phys. Lett. A **376**, 2200 (2012).

[21] L. E. Young-S., S. K. Adhikari, and P. Muruganandam, Phys. Rev. A **85**, 033619 (2012).

[22] A. G. Truscott *et al*., Science **291**, 2570 (2001).

[23] B. DeMarco and D. S. Jin, Science **285**, 1703 (1999).

[24] B. J. DeSalvo, M. Yan, P. G. Mickelson, Y. N. Martinez de Escobar, and T. C. Killian, Phys. Rev. Lett. **105**, 030402 (2010).

[25] M. W. Zwierlein *et al*., Nature (London) **435**, 7045 (2005).

[26] M. Greiner, C. A. Regal, and D. S. Jin, Nature (London) **426**, 537 (2003).

[27] M. Lu, N. Q. Burdick, and B. L. Lev, Phys. Rev. Lett. **108**, 215301 (2012).

[28] K.-K. Ni *et al*., Science **322**, 231 (2008); Nature (London) **464**, 1324 (2010).

[29] T. Lahaye *et al*., Rep. Prog. Phys. **72**, 126401 (2009).

[30] J.-N. Zhang and S. Yi, Phys. Rev. A **80**, 053614 (2009); T. Miyakawa, T. Sogo, and H. Pu, *ibid*. **77**, 061603 (2008); T. Sogo, L. He, T. Miyakawa, S. Yi, H. Lu, and H. Pu,

New J. Phys. **11**, 055017 (2009); B. Liu and L. Yin, Phys. Rev. A **84**, 053603 (2011).
[31] E. A. Donley, N. R. Claussen, S. L. Cornish, J. L. Roberts, E. A. Cornell, and C. E. Wieman, Nature (London) **412**, 295 (2001).
[32] S. K. Adhikari, Phys. Rev. A **66**, 013611 (2002).
[33] S. K. Adhikari, Phys. Rev. A **66**, 043601 (2002); J. Phys. B: At., Mol. Opt. Phys. **37**, 1185 (2004); Phys. Rev. E **65**, 016703 (2001).
[34] G. Modugno, G. Roati, F. Riboli, F. Ferlaino, R. J. Brecha, and M. Inguscio, Science **297**, 2240 (2002).
[35] S. K. Adhikari, Phys. Rev. A **70**, 043617 (2004).
[36] M. A. Baranov, L. Dobrek, and M. Lewenstein, Phys. Rev. Lett. **92**, 250403 (2004).
[37] L. Salasnich and F. Toigo, Phys. Rev. A **78**, 053626 (2008).
[38] A. R. P. Lima and A. Pelster, Phys. Rev. A **81**, 021606(R) (2010).
[39] S. K. Adhikari, Phys. Rev. A **72**, 053608 (2005).
[40] Luis E. Young-S. and S. K. Adhikari, Phys. Rev. A **87**, 013618 (2013).
[41] S. K. Adhikari and L. Salasnich, Phys. Rev. A **78**, 043616 (2008).
[42] S. K. Adhikari, Phys. Rev. A **77**, 045602 (2008); L. Salasnich, Laser Phys. **19**, 642 (2009); L. Salasnich, F. Ancilotto, and F. Toigo, Laser Phys. Lett. **7**, 78 (2010).
[43] C. F. von Weizsäcker, Z. Phys. **96**, 431 (1935); E. Zaremba and H. C. Tso, Phys. Rev. B **49**, 8147 (1994).
[44] P. Muruganandam and S. K. Adhikari, Comput. Phys. Commun. **180**, 1888 (2009); D. Vudragovic, I. Vidanovic, A. Balaz, P. Muruganandam, and S. K. Adhikari, *ibid*. **183**, 2021 (2012).
[45] S. K. Adhikari, Phys. Lett. A **346**, 179 (2005).
[46] S. K. Adhikari, Phys. Rev. A **63**, 043611 (2001).
[47] J. L. Roberts, N. R. Claussen, S. L. Cornish, and C. E. Wieman, Phys. Rev. Lett. **85**, 728 (2000).
[48] J. Stuhler, A. Griesmaier, T. Koch, M. Fattori, T. Pfau, S. Giovanazzi, P. Pedri, and L. Santos, Phys. Rev. Lett. **95**, 150406 (2005).